

Molecular Docking for the Development of Alternative Therapies against Leishmaniasis [†]

Juan Diego Guarimata ¹, Christian Alcívar ¹, Martín Lavecchia ^{2,*} and Ana Poveda ^{1,*}

¹ DNA Replication and Genome Instability Unit, Grupo de Investigación en Biodiversidad, Zoonosis y Salud Pública (GIBCIZ), Instituto de Investigación en Zoonosis-CIZ, Facultad de Ciencias Químicas, Universidad Central del Ecuador, Quito 170521, Ecuador; jdguarimata@uce.edu.ec (J.D.G.); cdalcivar@uce.edu.ec (C.A.)

² Centro de Química Inorgánica (UNLP, CCT-CONICET La Plata, Associated with CIC), Departamento de Química, Facultad de Ciencias Exactas, Universidad Nacional de La Plata, La Plata CP 1900, Argentina

* Correspondence: lavecchia@quimica.unlp.edu.ar (M.L.); apoveda@uce.edu.ec (A.P.); Tel.: +54-9-2214-95-7316 (M.L.); +593-99-987-1271 (A.P.)

[†] Presented at the 27th International Electronic Conference on Synthetic Organic Chemistry (ECSOC-27), 15–30 November 2023; Available online: <https://ecsoc-27.sciforum.net/>.

Abstract: Topoisomerases play a pivotal role in regulating the topological structure of DNA during fundamental processes such as transcription, DNA repair, or DNA replication; because of this, topoisomerases are biological targets in pathogenic microorganisms or malignant cells. In this study, we aimed to identify potential inhibitory compounds against topoisomerases type II of *Leishmania mexicana* via homology model and molecular docking. A comprehensive screening of 400 compounds provided by Medicines for Malaria Venture (MMV) in the Pandemic Response Box. Here, we identify the 20 best compounds against each topoisomerase type II of *L. mexicana* to identify new alternatives to treat a neglected tropical disease such as leishmaniasis.

Keywords: *Leishmania mexicana*; topoisomerase; molecular docking; homology modeling; neglected tropical disease



Citation: Guarimata, J.D.; Alcívar, C.; Lavecchia, M.; Poveda, A. Molecular Docking for the Development of Alternative Therapies against Leishmaniasis. *Chem. Proc.* **2023**, *14*, 82. <https://doi.org/10.3390/ecsoc-27-16050>

Academic Editor: Julio A. Seijas

Published: 15 November 2023



Copyright: © 2023 by the authors. Licensee MDPI, Basel, Switzerland. This article is an open access article distributed under the terms and conditions of the Creative Commons Attribution (CC BY) license (<https://creativecommons.org/licenses/by/4.0/>).

1. Introduction

Leishmaniasis is a neglected tropical disease constituting a public health problem in the Americas due to its high incidence, morbidity, wide geographical distribution and variety of parasite species and clinical forms, as well as a lack of adequate therapeutic and prevention measures [1]. Ecuador is an endemic area for cutaneous leishmaniasis caused by *L. mexicana* with around 900 annual cases [2]. The drugs currently employed for leishmaniasis treatment exhibit limited efficacy in advanced stages, lack specificity, and are often associated with high toxicity [1]. Finding alternative drugs to effectively treat and control these diseases is therefore a priority.

The current increase in microbial resistance is a very serious public health problem that requires immediate attention from governments and the scientific community, among others [3]. The Pandemic Response Box (PRB) is a collection of 400 pre-synthesized compounds to facilitate drug discovery provided by Medicines for Malaria Venture (MMV) www.mmv.org (accessed on 28 February 2023) [4]. The collection contains chemically characterized compounds that are freely available to the scientific community. Computational tools including molecular docking have allowed enormous progress in the discovery of new drugs by focusing experimental trials on promising compounds, improving efficiency in terms of time and money in the search for therapeutic alternatives [5]. Type II topoisomerases are enzymes that control changes in DNA topology by catalyzing a controlled breakage and resealing of DNA strands, alleviating the excess of supercoiling [6]. Interference with the normal functioning of this types of enzymes becomes the mechanism of action of antibacterial drugs such as fluoroquinolones or anticancer drugs such as etoposide,

leading to cell death [6,7]. *L. mexicana* has two type II topoisomerases, one located in the nucleus and another in the kinetoplast, a giant and unique mitochondria characteristic of these parasites [8,9].

We report the 20 best candidates to inhibit each of the type II topoisomerases of *L. mexicana* via molecular docking carried out using the software FRED v4.2.1.0 (Chemgauss4), comparing beforehand the performance of three virtual screening methods (Autodock Vina v1.2.0, FRED and HYBRID v4.2.1.0 (Chemgauss4)) to discern between decoys and active molecules in molecular docking against human beta topoisomerase II (hTopII beta) (RCSB-PDB accession code: 3QX3). We implemented receiver operating characteristics (ROC) curves as a tool to compare the predictive power of the three virtual screening methods tested.

2. Materials and Methods

2.1. Sequence Retrieval, Homology Modeling, and Refinement

Both topoisomerases type II from *L. mexicana* were modeled due to the absence of X-ray crystallography of these proteins for the species. The amino acid sequences of nuclear topoisomerase (nuclear TopII) and mitochondrial topoisomerase (mitochondrial TopII) retrieved from NCBI with the accession numbers “XP_003877071.1” and “XP_003873648.1”, respectively, were selected for this study. Homology modeling was implemented via SWISS-MODEL “<http://swissmodel.expasy.org> (accessed on 3 March 2023)”, by extrapolating the experimental information from related protein structures that served as a template [10]. Specifically, the most effective models were constructed using a *Saccharomyces cerevisiae* topoisomerase template (PDB accession code: 4gfh.1). These models, demonstrating 46.20% sequence identity for nuclear TopII and 32.72% for mitochondrial TopII, were then saved in PDB format.

Before virtual screening, DNA chains, magnesium as co-factors and etoposide as ligand were added to mitochondrial and nuclear TopII of *L. mexicana* by extracting them from hTopII beta (PDB accession code: 3QX3) and human alpha topoisomerase (hTopII alpha) (PDB accession code: 5GWK), respectively. A minimization was run using NAMD2 v2.14 to refine the modeled structures, using amber force field DNA.OL15 (DNA), FF14SB (protein) and GAFF (EVP). The topology was prepared using Leap, included in AmberTools v22. The minimization consisted of a series of steps: hydrogen minimization, water minimization, side chain minimization and full structure minimization. All the minimization steps allowed the structure to relax and no atoms to overlap.

2.2. Binding Site Determination

To generate the grid box coordinates needed for virtual screening with Autodock Vina, a sequence alignment was created using the MultAlin tool “<http://multalin.toulouse.inra.fr/multalin/multalin.html> (accessed on 22 March 2023)” [11], between the hTopIIbeta (NCBI accession code: NP_001317629.1) and the parasitic topoisomerases (accession codes above), which allowed the identification of homologous residues between these topoisomerases, with emphasis on the catalytic residues present in hTopIIbeta (P819; Y821) as well as the binding residues to etoposide (P501; L502; R503; E522; G776; E777; Q778; A779; M782; A816) [12,13]. To define the binding pocket for hTopIIbeta, ADT from MGLTools v1.5.7 was used [14], and the following coordinates were generated: center_x = 30.41, center_y = 99.699, center_z = 43.198, size_x = 32, size_y = 34, size_z = 34. In the case of HYBRID and FRED, the active site was selected around etoposide.

2.3. Receiver Operating Characteristic (ROC) Curves

To generate the ROC curves, it was necessary to have active compounds against hTopII beta; these compounds were obtained from the ChEMBL platform “<https://www.ebi.ac.uk/chembl/> (accessed on 3 May 2023)” [15], where compounds with a pChEMBL value of 5.5 to 8.26 were selected [16]. The decoys needed for the ROC curve were generated with the active compounds via DUD-E “<https://dude.docking.org/> (accessed on 3 May 2023)” [17], obtaining 50 decoys per active molecule. Molecular docking was carried out

with 500 molecules, about 25 actives molecules and 475 decoys. Three software were used (Autodock Vina v1.2.0 [18], HYBRID and FRED v4.2.1.1 suite [19]) and the ROC curves and ROC AUCs were generated using the Screening Explorer tools “<http://stats.drugdesign.fr/>” (accessed on 14 June 2023) [20].

2.4. MMV Ligand Preparation and Molecular Docking

Once the ROC curves were created, the software FRED was used to complete the molecular docking with etoposide, the ligands of MMV, hTopII beta, hTopII alpha and the topoisomerases type II of *L. mexicana*, based on the ROC AUCs for this software. First, the SMILES codes of all the ligands (400) given by MMV and the SMILE code for etoposide taken from Pubchem (PubChem CID: 36462) “<https://pubchem.ncbi.nlm.nih.gov/>” (accessed on 15 June 2023) [21]. were convert to 3D structures, protonate at pH 7.4, and minimize with a UFF force field [22], and with a subsequent transformation of all molecules into .pdbqt format. The Kollman charges of the proteins of *L. mexicana* and human topoisomerases isoenzymes were added with MGLTools v1.5.7, and the proteins were saved in the format .pdbqt. Finally, molecular docking was carried out between the 401 molecules against each topoisomerase.

2.5. Interactions

The analysis of the four docking results was carried out using Discovery Studio Visualizer v21.1.0.20298 [23].

3. Results

In the alignment carried out between the human and leishmania topoisomerases (not shown), the residues involved in binding with etoposide in hTopII beta (P501; L502; R503) are conserved in all topoisomerases; additionally, the residues also involved in binding with etoposide (G776; E777; Q778), the residue Q778 is only conserved in the nuclear TopII of *L. mexicana*, however, it is changed for a non-polar residue in hTopII alpha (M762) and changed for another non-polar residue in mitochondrial TopII (A732). Residues G776 and E777 are conserved in all topoisomerases. Conversely, the catalytic residues of hTopII beta (P819, Y821) are conserved in all topoisomerases, except in nuclear TopII, where P819 is replaced with another non-polar residue, G769.

Figure 1 shows the three ROC curves of the three virtual screening methods implemented made with 475 decoys and 25 active molecules against hTopIIbeta.

Table 1 shows the 20 best free energy binding results of molecular docking using the software FRED (each topoisomerase II of *L. mexicana* and each human topoisomerase isoenzyme against MMV ligands). EVP was added to compare the binding energy between the ligands and this molecule. The software FRED was selected for the virtual screening based on the predictive power detected using the ROC curve.

Figure 2 shows the chemical structure of ligand058, which exhibits binding to the nuclear TopII and mitochondrial TopII of *L. mexicana* but not to the human topoisomerases; the chemical structure of etoposide is also shown to compare.

Figure 3 shows the different forms of binding between ligand058 and nuclear TopII or hTopIIbeta.

Table 1. 20 best binding energies between each topoisomerase evaluated and ligands of MMV; also shows the binding energy of etoposide with these topoisomerases.

Nuclear TopII <i>L. mexicana</i>		Mitochondrial TopII <i>L. mexicana</i>		hTopII Alpha		hTopII Beta	
Ligand ID	Score	Ligand ID	Score	Ligand ID	Score	Ligand ID	Score
058	−17.895	389	−19.766	046	−19.840	etoposide	−19.884
363	−17.140	280	−18.509	180	−19.413	208	−19.522
091	−17.040	301	−18.232	170	−19.073	070	−19.056

Table 1. Cont.

Nuclear TopII <i>L. mexicana</i>		Mitochondrial TopII <i>L. mexicana</i>		hTopII Alpha		hTopII Beta	
389	-16.610	058	-18.069	108	-18.996	288	-19.026
050	-16.560	151	-18.059	190	-18.892	364	-18.824
313	-16.516	155	-17.960	290	-18.813	040	-18.700
296	-16.440	128	-17.949	363	-18.519	180	-18.478
191	-16.228	269	-17.916	373	-18.497	280	-18.428
192	-16.172	091	-17.845	280	-18.445	091	-18.411
354	-16.126	078	-17.775	040	-18.409	108	-18.347
016	-16.072	187	-17.567	288	-18.392	37	-18.151
280	-15.930	363	-17.448	etoposide	-18.381	190	-18.059
326	-15.892	344	-17.422	078	-18.316	016	-17.991
134	-15.817	386	-17.391	016	-18.263	397	-17.951
204	-15.705	205	-17.366	389	-18.255	043	-17.875
376	-15.667	133	-17.317	023	-18.224	335	-17.870
133	-15.591	195	-17.313	091	-18.096	065	-17.826
370	-15.586	288	-17.302	333	-18.079	023	-17.794
288	-15.494	399	-17.177	070	-18.022	373	-17.713
048	-15.467	100	-17.158	138	-17.987	333	-17.674
etoposide	-13.252	etoposide	-15.270	168	-17.983	100	-17.588

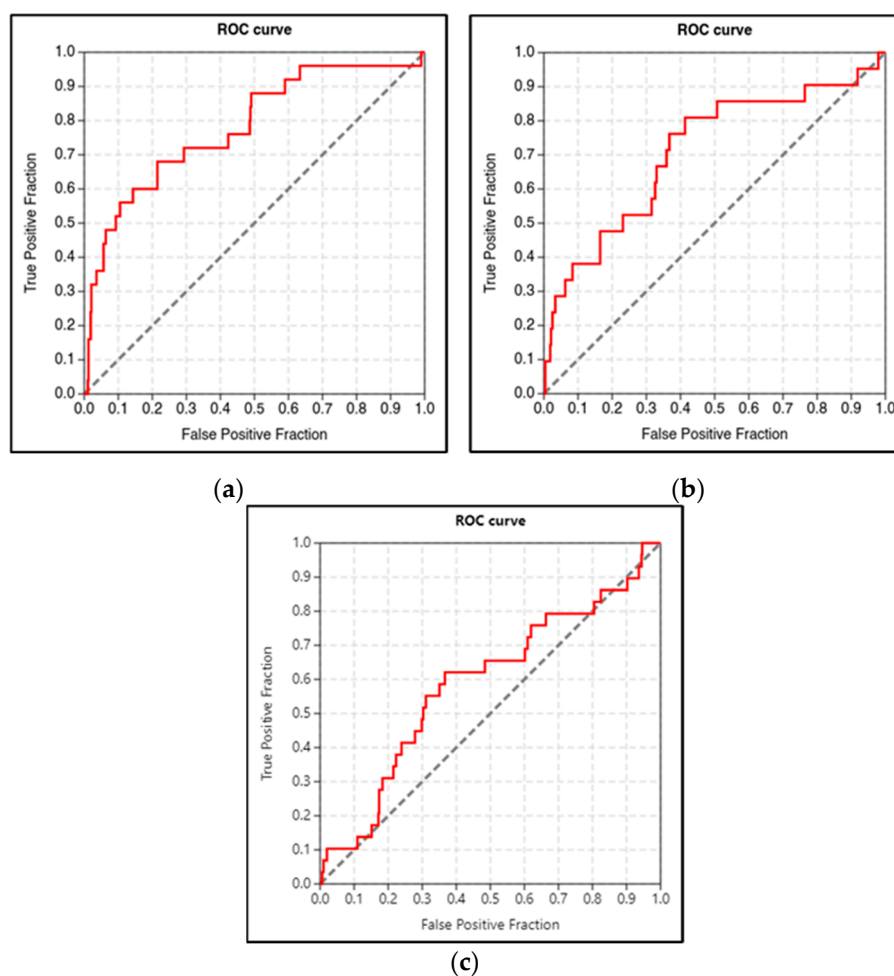


Figure 1. ROC curves for each docking software: (a) ROC curve for FRED software, ROC AUC: 0.780; (b) ROC curve for HYBRID software, ROC AUC: 0.710; (c) ROC curve for AutoDock Vina software, ROC AUC: 0.589.

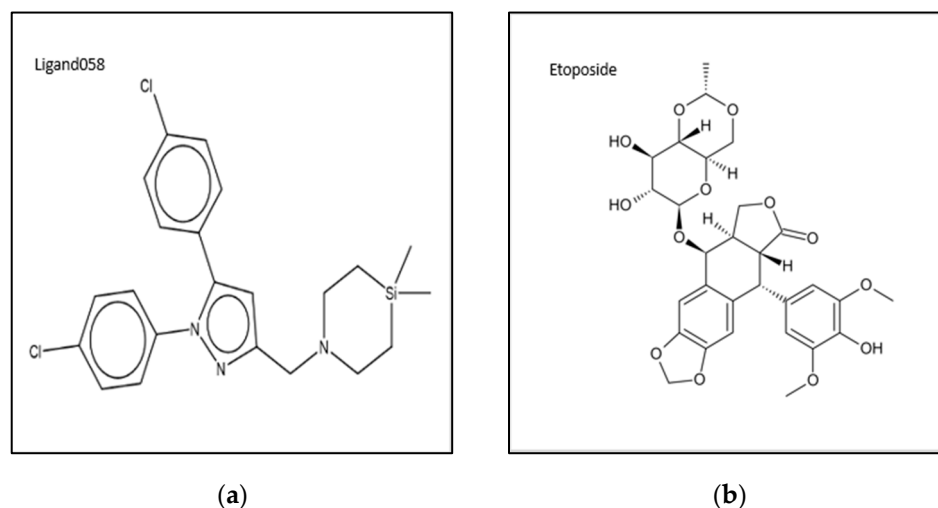


Figure 2. Chemical structure of molecules: (a) ligand058 only selective for type II *L. mexicana* topoisomerases; (b) etoposide.

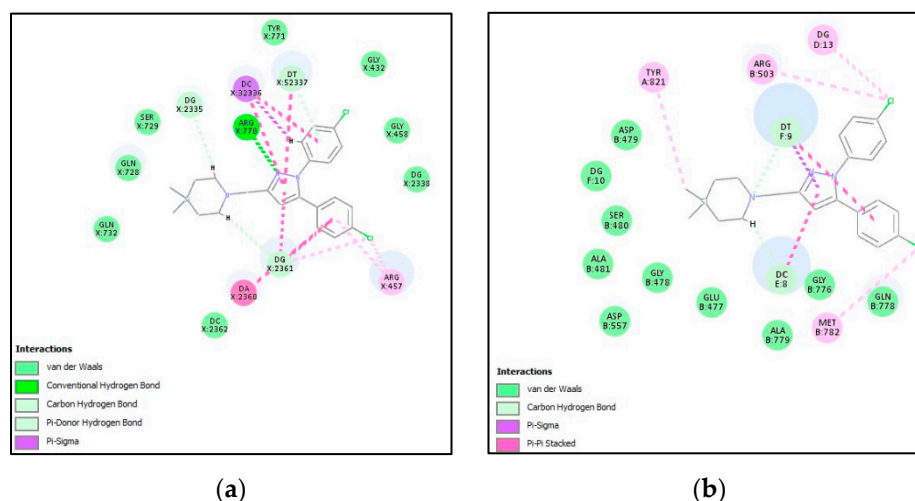


Figure 3. Binding between nuclear TopII and hTopIIbeta with ligand058: (a) nuclear TopII/058; (b) hTopII beta/058.

4. Discussion

This study employs molecular docking to identify the top 25 compounds from the Medicines for Malaria Venture's (MMV) Pandemic Response Box as potential inhibitors of Topoisomerase II (TopII) in *L. mexicana*. The implemented receiver ROC curves shown in Figure 1 demonstrated that the FRED software has the best capacity to distinguish between active and inactive compounds to screen databases with accuracy among the software tested, which allows the identification of candidates in a time-efficient and cost-effective manner; however, this does not imply that experimental confirmation of hits will occur [18].

Table 1 shows that the 25 best compounds selective only to *L. mexicana* topoisomerases have higher binding energy than etoposide, perhaps due to the presence of imidazole, pyridine, pyrimidine, benzimidazole and piperidine rings among the ligands, unlike etoposide, shown in Figure 2. These rings allowed hydrogen bonds with key residues such as Arg770 as an example with 058 in Figure 3; this is possibly due to nitrogen heterocycles rich in electrons exhibiting a notable capacity to easily accept or donate electrons, allowing them to engage in a wide range of weak interactions and readily attach to various therapeutic targets [24,25]. The ring skeletons mentioned above would be excellent pharmacophores for developing TopII inhibitors for targeted leishmaniasis therapy. On the other hand, halogens, especially chlorine and fluorine, encountered in most of the best ligands (Figure 2), have a

beneficial impact on the biological characteristics of molecules via halogen bonding. This bonding has been identified as one of the mechanisms by which chlorine and fluorine modify the biological effects of molecules [26].

By reviewing the scores obtained for etoposide and the ligands against the evaluated topoisomerases, it is expected that etoposide will serve as a drug to validate the computational method in vitro since human topoisomerases should be more sensitive to etoposide than topoisomerases from *L. mexicana*. Based on this, tests are being carried out in the laboratory with human monocytes (THP-1) [27] and with *L. mexicana* (bel 21), as a starting point to test the found hits and complete our objective of identifying new alternatives to treat a neglected tropical disease such as leishmaniasis.

Author Contributions: Conceptualization, A.P.; methodology, J.D.G., M.L., A.P. and C.A.; software, J.D.G. and M.L.; validation, J.D.G. and M.L.; formal analysis, M.L. and A.P.; writing—original draft preparation, J.D.G.; writing—review and editing, A.P.; visualization, M.L. and C.A. All authors have read and agreed to the published version of the manuscript.

Funding: This research received no external funding.

Institutional Review Board Statement: Not applicable.

Informed Consent Statement: Not applicable.

Data Availability Statement: Not applicable.

Conflicts of Interest: The authors declare no conflicts of interest.

References

1. Pradhan, S.; Schwartz, R.A.; Patil, A.; Grabbe, S.; Goldust, M. Treatment options for leishmaniasis. *Clin. Exp. Dermatol.* **2022**, *47*, 516–521. [CrossRef] [PubMed]
2. Dirección Nacional de Vigilancia Epidemiológica. Available online: https://www.salud.gov.ec/wp-content/uploads/2023/02/Gaceta-SE-1_2023.pdf (accessed on 24 August 2023).
3. Laws, M.; Shaaban, A.; Rahman, K.M. Antibiotic resistance breakers: Current approaches and future directions. *FEMS Microbiol. Rev.* **2019**, *43*, 490–516. [CrossRef] [PubMed]
4. MMV. Available online: <https://www.mmv.org/mmv-open/pandemic-response-box/about-pandemic-response-box> (accessed on 14 July 2023).
5. Stanzione, F.; Giangreco, I.; Cole, J.C. Use of molecular docking computational tools in drug discovery. *Prog. Med. Chem.* **2021**, *60*, 273–343. [CrossRef] [PubMed]
6. Economides, M.P.; McCue, D.; Borthakur, G.; Pemmaraju, N. Topoisomerase II inhibitors in AML: Past, present, and future. *Expert. Opin. Pharmacother.* **2019**, *20*, 1637–1644. [CrossRef] [PubMed]
7. Pommier, Y.; Leo, E.; Zhang, H.; Marchand, C. DNA topoisomerases and their poisoning by anticancer and antibacterial drugs. *Chem. Biol.* **2010**, *17*, 421–433. [CrossRef] [PubMed]
8. Cortázar, T.M.; Coombs, G.H.; Walker, J. Leishmania panamensis: Comparative inhibition of nuclear DNA topoisomerase II enzymes from promastigotes and human macrophages reveals anti-parasite selectivity of fluoroquinolones, flavonoids and pentamidine. *Exp. Parasitol.* **2007**, *116*, 475–482. [CrossRef]
9. Das, B.B.; Ganguly, A.; Majumder, H.K. DNA topoisomerases of Leishmania: The potential targets for anti-leishmanial therapy. *Adv. Exp. Med. Biol.* **2008**, *625*, 103–115. [CrossRef]
10. Waterhouse, A.; Bertoni, M.; Bienert, S.; Studer, G.; Tauriello, G.; Gumienny, R.; Heer, F.T.; de Beer, T.A.P.; Rempfer, C.; Bordoli, L.; et al. SWISS-MODEL: Homology modelling of protein structures and complexes. *Nucleic Acids Res.* **2018**, *46*, 296–303. [CrossRef]
11. Corpet, F. Multiple sequence alignment with hierarchical clustering. *Nucleic Acids Res.* **1988**, *16*, 10881–10890. [CrossRef]
12. Wu, C.C.; Li, Y.C.; Wang, Y.R.; Li, T.K.; Chan, N.L. On the structural basis and design guidelines for type II topoisomerase-targeting anticancer drugs. *Nucleic Acids Res.* **2013**, *41*, 10630–10640. [CrossRef]
13. Wendorff, T.J.; Schmidt, B.H.; Heslop, P.; Austin, C.A.; Berger, J.M. The structure of DNA-bound human topoisomerase II alpha: Conformational mechanisms for coordinating inter-subunit interactions with DNA cleavage. *J. Mol. Biol.* **2012**, *424*, 109–124. [CrossRef] [PubMed]
14. Sanner, M. Python: A Programming Language for Software Integration and Development. *J. Mol. Graph. Mod.* **1999**, *17*, 57–61.
15. Mendez, D.; Gaulton, A.; Bento, A.P.; Chambers, J.; De Veij, M.; Félix, E.; Magariños, M.P.; Mosquera, J.F.; Mutowo, P.; Nowotka, M.; et al. ChEMBL: Towards direct deposition of bioassay data. *Nucleic Acids Res.* **2019**, *47*, D930–D940. [CrossRef] [PubMed]
16. Assay and Activity Questions. Available online: <https://chembl.gitbook.io/chembl-interface-documentation/frequently-asked-questions/chembl-data-questions> (accessed on 14 July 2023).

17. Mysinger, M.M.; Carchia, M.; Irwin, J.J.; Shoichet, B.K. Directory of useful decoys, enhanced (DUD-E): Better ligands and decoys for better benchmarking. *J. Med. Chem.* **2012**, *55*, 6582–6594. [[CrossRef](#)]
18. Eberhardt, J.; Santos-Martins, D.; Tillack, A.F.; Forli, S. AutoDock Vina 1.2.0: New Docking Methods, Expanded Force Field, and Python Bindings. *Chem. Inf. Model.* **2021**, *61*, 3891–3898. [[CrossRef](#)]
19. McGann, M. FRED and HYBRID docking performance on standardized datasets. *J. Comput. Aided Mol. Des.* **2012**, *26*, 897–906. [[CrossRef](#)]
20. Empereur-Mot, C.; Zagury, J.F.; Montes, M. Screening Explorer-An Interactive Tool for the Analysis of Screening Results. *J. Chem. Inf. Model.* **2016**, *56*, 2281–2286. [[CrossRef](#)]
21. Kim, S.; Chen, J.; Cheng, T.; Gindulyte, A.; He, J.; He, S.; Li, Q.; Shoemaker, B.A.; Thiessen, P.A.; Yu, B.; et al. PubChem 2023 update. *Nucleic Acids Res* **2023**, *51*, D1373–D1380. [[CrossRef](#)]
22. O’Boyle, N.M.; Banck, M.; James, C.A.; Morley, C.; Vandermeersch, T.; Hutchison, G.R. Open Babel: An open chemical toolbox. *J. Cheminf.* **2011**, *3*, D1373–D1380. [[CrossRef](#)]
23. BIOVIA Discovery Studio-Dassault Systèmes. Available online: <https://www.3ds.com/products-services/biovia/products/molecular-modeling-simulation/biovia-discovery-studio/> (accessed on 13 October 2023).
24. Bhatnagar, A.; Sharma, P.K.; Kumar, N. A review on “Imidazoles”: Their chemistry and pharmacological potentials. *Int. J. PharmTech Res.* **2011**, *3*, 268–282.
25. Ingle, R.G.; Magard, D. Heterocyclic chemistry of benzimidazoles and potential activities of derivatives. *Int. J. PharmTech Res.* **2011**, *1*, 26–32.
26. Sirimulla, S.; Bailey, J.B.; Vegesna, R.; Narayan, M. Halogen interactions in protein-ligand complexes: Implications of halogen bonding for rational drug design. *J. Chem. Inf. Model.* **2013**, *53*, 2781–2791. [[CrossRef](#)] [[PubMed](#)]
27. Chanput, W.; Mes, J.J.; Wichers, H.J. THP-1 cell line: An in vitro cell model for immune modulation approach. *Int. Immunopharmacol.* **2014**, *23*, 37–45. [[CrossRef](#)] [[PubMed](#)]

Disclaimer/Publisher’s Note: The statements, opinions and data contained in all publications are solely those of the individual author(s) and contributor(s) and not of MDPI and/or the editor(s). MDPI and/or the editor(s) disclaim responsibility for any injury to people or property resulting from any ideas, methods, instructions or products referred to in the content.